Sputtering power and deposition pressure effects on the electrical and structural properties of copper thin films

KAH-YOONG CHAN*, BEE-SAN TEO
Faculty of Engineering, Multimedia University, Jalan Multimedia, 63100 Cyberjaya, Selangor, Malaysia
E-mail: cy_38@yahoo.com

Published online: 8 September 2005

We investigated the effects of sputtering power and deposition pressure on the electrical and structural properties of dc magnetron sputter-deposited copper films on *p*-type silicon grown at room temperature. Results from our experiments showed that the deposition rate of the copper films increased proportionally with the sputtering power. Sputtering power also affected the structural properties of the copper films through the surface diffusion mechanism of the adatom. From the scanning electron microscopy surface analysis, the high sputtering power favored the formation of continuous film. The poor microstructure with voided boundaries as a result of low sputtering power deposition was manifested with the high resistivity obtained. The deposition rate was found also depending on the deposition pressure. The deposition pressure had the contrary effect on structural properties of copper films in which high deposition pressure favored the formation of voided boundaries film structure due to the shadowing effect, which varied with different deposition pressure. © *2005 Springer Science + Business Media, Inc.*

1. Introduction

The increasing demand for miniaturization of electronic devices has stimulated research in thin film. Basic scientific concern is focussed on film formation processes in order to obtain the insight into mechanism leading to special structural properties. It is, however, not only the film structure but also the thickness, which determines the physical properties of the thin film. The challenges in the thin film research thus lie in the optimization of the thin film properties of required thickness under various deposition techniques to tailor for specific application.

Copper (Cu) thin films with sub-micron geometric and microstructural dimensions have been used in modern applications ranging from catalysis to microelectronic devices. In ultralarge scale integrated circuits (ULSI), achievement of maximum signal transmission in emerging chip and system architectures requires minimizing the resistance-capacitance (RC) time delay. RC delay has replaced intrinsic device delay as the major speed limiter in sub-micron device, due primarily to the increasingly higher RC time constant in the ever narrower, more closely spaced interconnect lines. Minimizing RC delay in thinner interconnects has forced a transition from aluminum (Al) based interconnects to Cu metallization schemes owing to the higher conductance of Cu, which not only reduces the delay time but also enables higher current densities at lower voltages, minimizing heat generation and power requirements and increasing the packaging densities per metallization level. Apart from reduction in RC time delay, Cu is more promising than Al for metallization in terms of electromigration resistance and mechanical elasticity stress [1]. Cu exhibits superior resistance to electromigration as its atoms are more strongly bounded together which account for less likely to fracture under stress comparing to Al.

The study of Cu thin film is generally centered on the electrical and microstructural properties as well as the crystallinity and texture of the Cu films deposited with various deposition techniques. Among these, evaporation [2], sputtering [3–5], chemical vapor deposition [6], metal organic chemical vapor deposition [7], electroplating [8] and partially ion beam (PIB) techniques [9–11] are being used for Cu film deposition and have been reported. In the present study, we investigated the electrical and structural properties of DC magnetron sputter-deposited Cu films on *P*-type Si substrates under various deposition conditions. In addition to these, we also examined the surface morphology of the Cu thin films grown at different power and pressure.

*Author to whom all correspondence should be addressed.

0022-2461 © *2005 Springer Science + Business Media, Inc.*
DOI: 10.1007/s10853-005-1362-8

2. Experimental

All Cu films were deposited in a DC magnetron sputtering deposition chamber with base pressure lower than 5×10^{-6} Torr. The Cu target was of 99.995% purity. The Argon (Ar), which was used as process gas was 99.995% pure and the substrates used were (100) *P*-type Si. The Si substrates geometry was approximately 6 mm (W) × 12 mm (L) and were kept at room temperatures during the deposition. The magnetron cathode was placed at a distance of about 9 cm from the substrate holder. The thickness of the deposited Cu films was checked by a quartz crystal monitor during the sputtering process, and was quantified with the Mahr surface profilometer after the process. LEO 1450VP scanning electron microscopy was used to examine the surface morphology of the Cu films grown at different conditions. The film resistance was measured with Karl Suss four-point probe. The growth details for three sets of experiments to study the sputtering power and deposition pressure dependent electrical and structural properties were tabulated in Table I.

TABLE I Cu films growth details

Exp.	Dep. Pres (m Torr)	Sput power (W)	Dep. time (min)
		Set 1	
Sample 1	3.6	25	10
Sample 2	3.6	50	10
Sample 3	3.6	75	10
Sample 4	3.6	100	10
Sample 5	3.6	125	10
Sample 6	3.6	150	10
		Set 2	
Sample 1	3.6	125	1.5
Sample 2	3.6	125	2.5
Sample 3	3.6	125	5
Sample 4	3.6	125	15
Sample 5	3.6	125	20
Sample 6	3.6	125	25
Sample 7	3.6	125	30
		Set 3	
Sample 1	1	100	10
Sample 2	3.6	100	10
Sample 3	5	100	10
Sample 4	10	100	10
Sample 5	20	100	10
Sample 6	30	100	10

3. Results and discussion

3.1. Sputtering power effects on structural and electrical properties

Fig. 1 shows deposition rate increases linearly proportionate with the sputtering power. We attribute this dependence relationship to the determinacy of sputter deposition rate on the Ar ion flux (J_{ion}) and its average kinetic energy (KE_{av}) upon striking the target. These are function of DC applied voltage (V_{dc}), according to Langmuir-Child Relationship [12a] and average kinetic energy equation in dc glow discharge [13];

$$J_{ion} \propto V_{dc}^{3/2} \quad (1)$$

$$KE_{av} \propto V_{dc} \quad (2)$$

The high Ar ion flux generally results in substantial ion bombardment on the target while the high kinetic energy of these ions increases the probability that the impacts of incident ions will eject target atoms. These two mechanisms are proportional to DC applied voltage and sputtering power, and hence contribute to the increase of the sputter deposition rate. Similar dependence relationship between deposition rate and sputtering power was reported by Gagaoudakis *et al.* [14] and Song *et al.* [15a]. Gagaoudakis *et al.* in particular attributed the dependence relationship to the increase of the flux of the sputtered particles with the increase of sputtering current.

Fig. 2 shows the plane view of SEM micrographs of Cu layer grown at 25, 50, 75, 100, 125, and 150 W

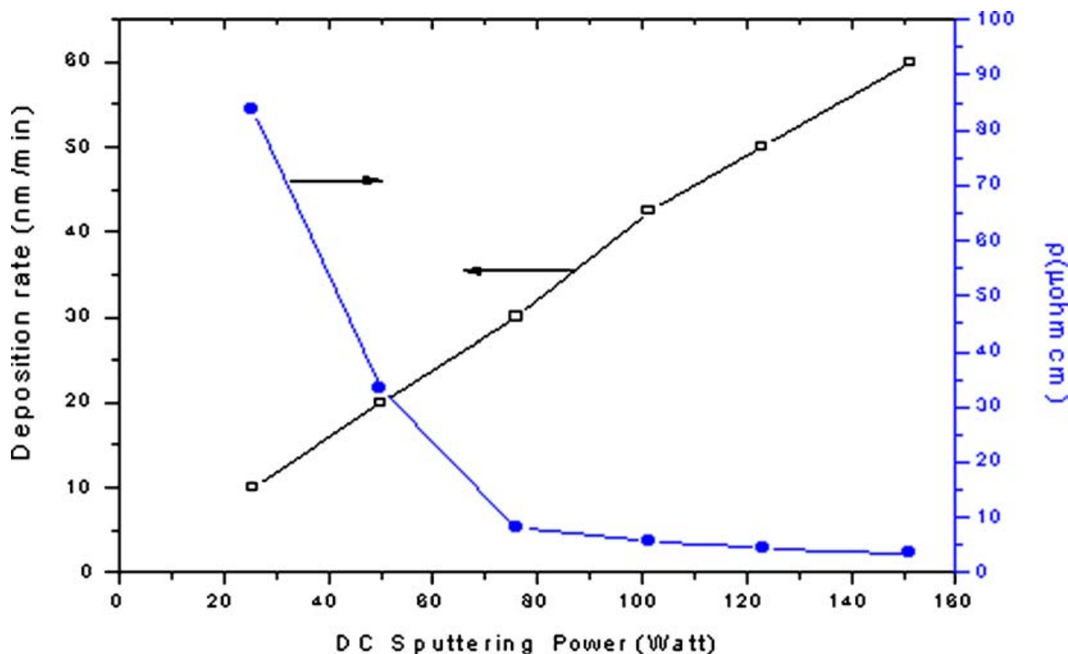

Figure 1 Sputtering power effects on the deposition rate and film resistivity at deposition pressure of 3.6 mTorr.

on silicon substrate at room temperature with the deposition pressure of 3.6 mTorr. The micrographs show that the Cu films exhibit crack-like structure prior to the increase of sputtering power to 100 W. Thereafter, fine round features develop in the Cu films and are enhanced with the increase in sputtering power. The cracks in Fig. 2a–c are voided boundaries, as observed by Joh *et al*. [16]. Based on their investigation on the microstructure of Cu films using high resolution SEM, they reported similar crack-like Cu film structure grown under low deposition pressure as voided boundaries due to shadowing effects. The voided boundaries observed

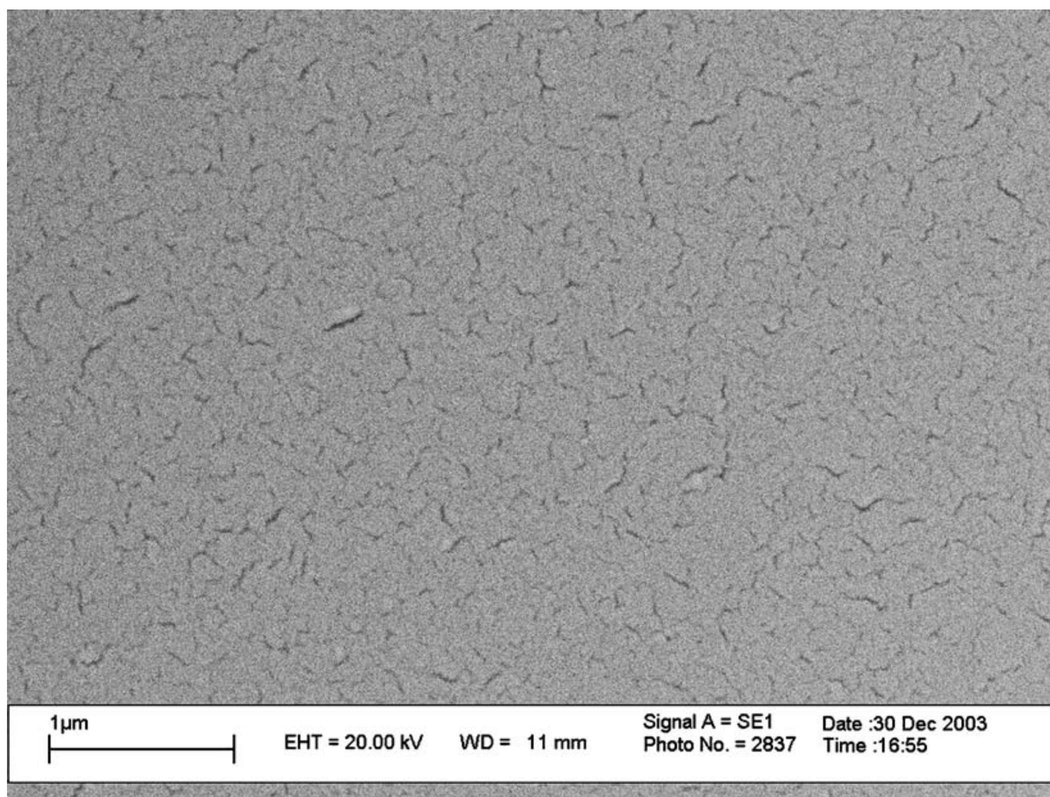

(a)

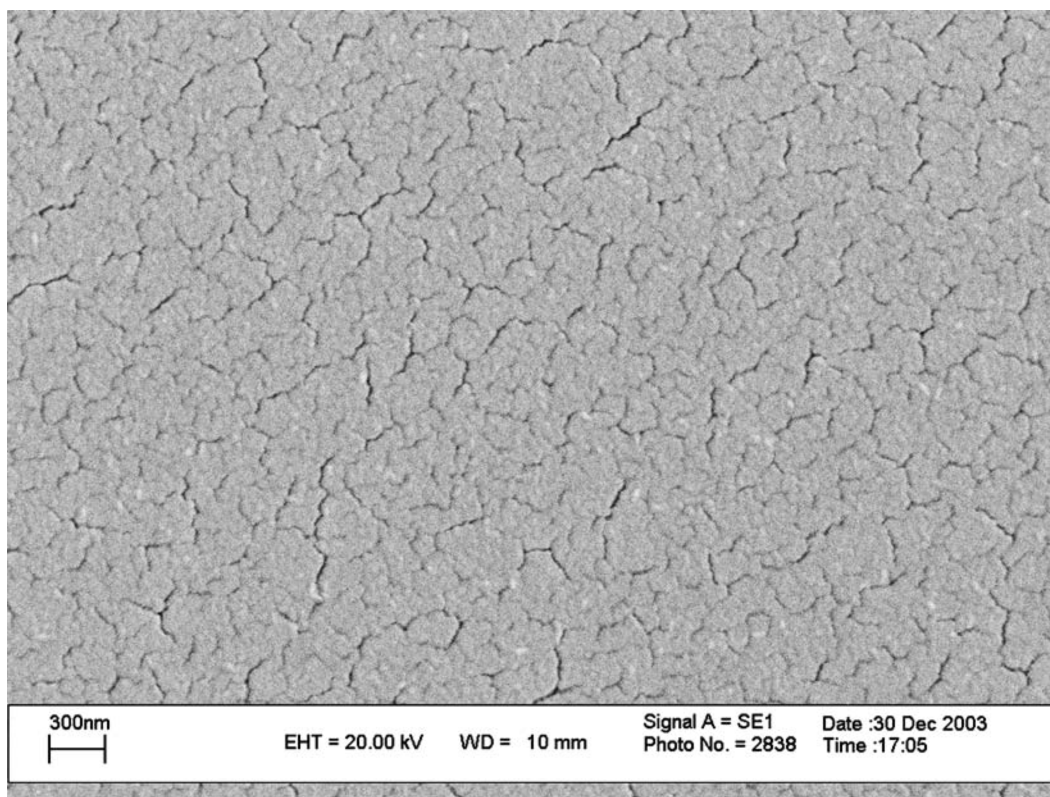

(b)

Figure 2 Plane view of SEM micrographs of Cu layer grown at: (a) 25 W, (b) 50 W, (c) 75 W, (d) 100 W, (e) 125 W, (f) 150 W on silicon substrate. (Magnification = 20.00 KX). (*Continued on next page*).

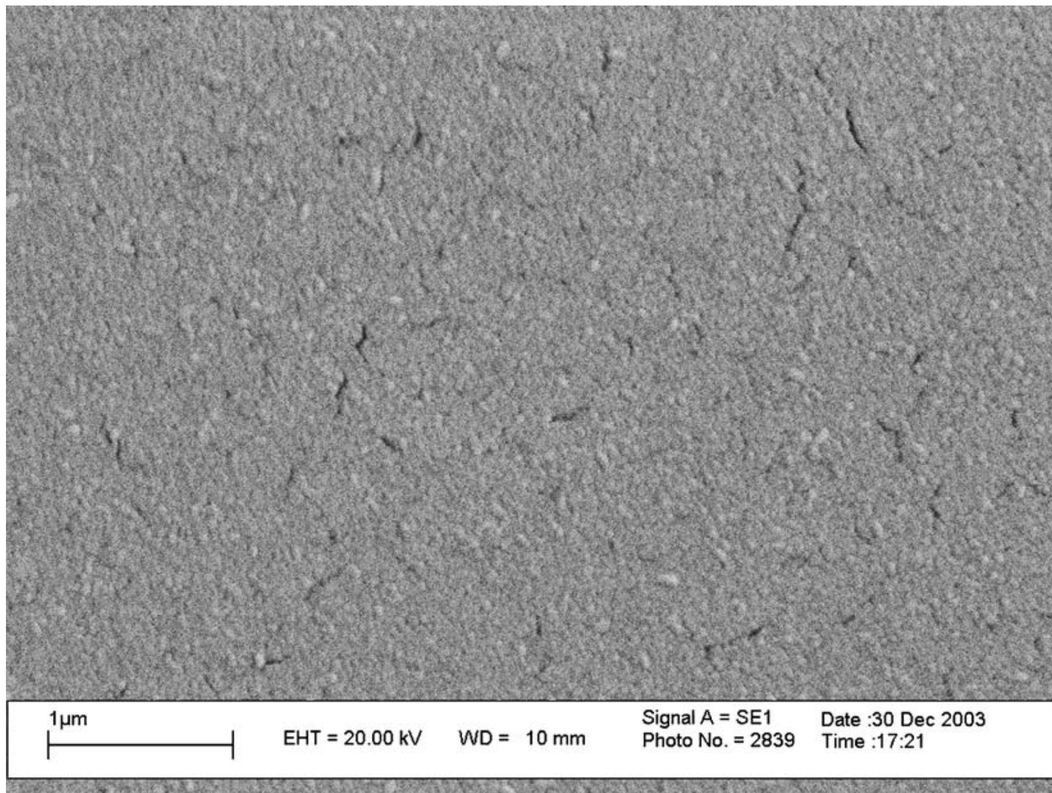

(c)

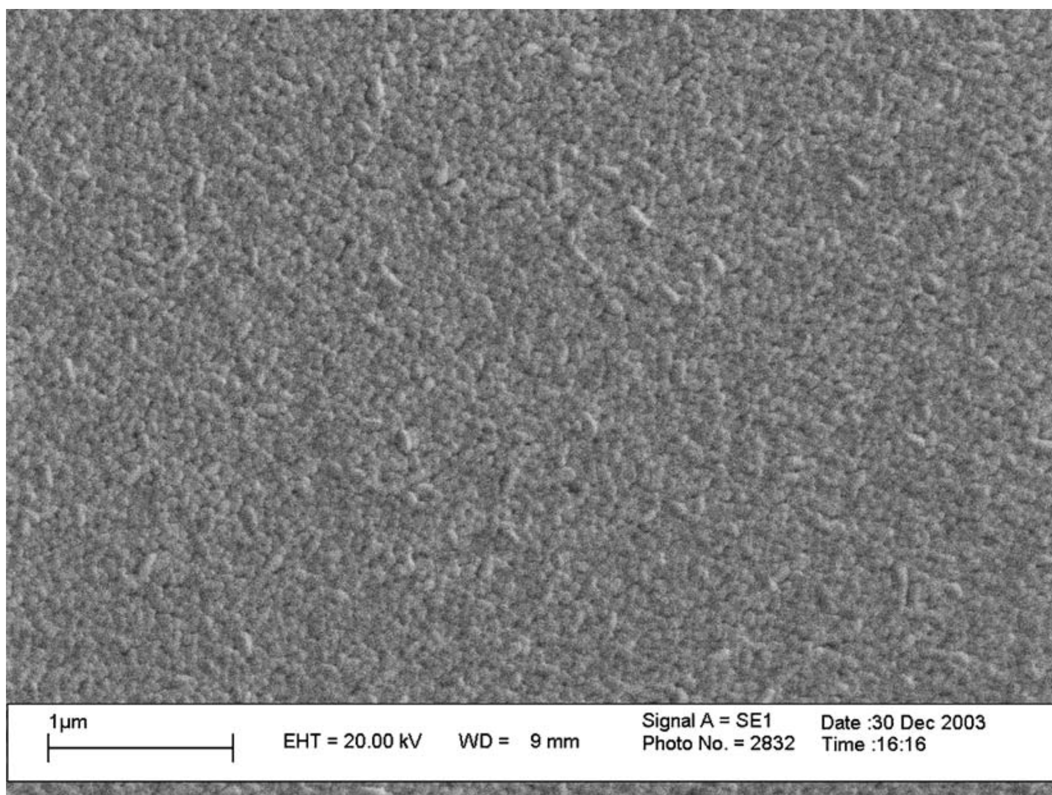

(d)

Figure 2 (*Continued*).

in Fig. 2 decrease as sputtering power increases. The voided boundaries in Fig. 2a at 25 W appear to be denser than Fig. 2b at 50 W, while the micrograph in Fig. 2c of 75 W shows less voided boundaries on film surface. The higher sputtering power giving less voided boundaries as observed in Fig. 2 is due to the fact that sputtering power helps to increase the surface mobility [17, 18a], which is required to form continuous film [12b]. The Cu adatoms, which are absorbed when they are deposited on the substrate surface may diffuse along the surface (surface diffusion), hopping from valley to valley in the surface potential. During

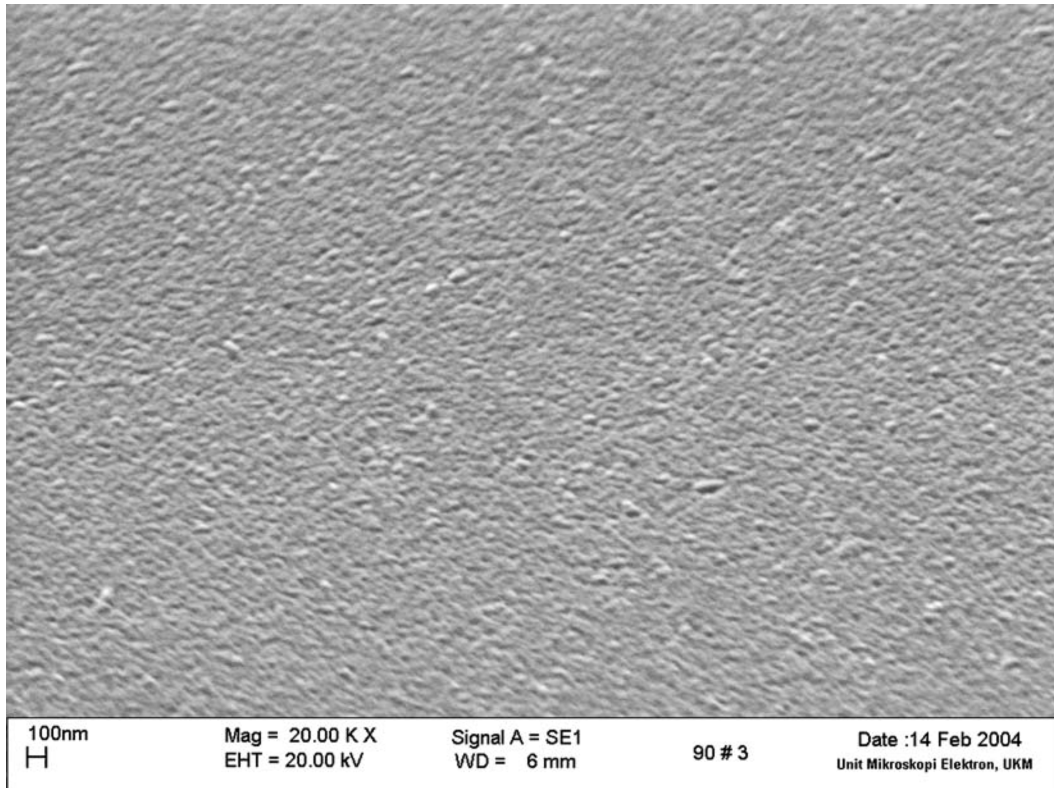

(e)

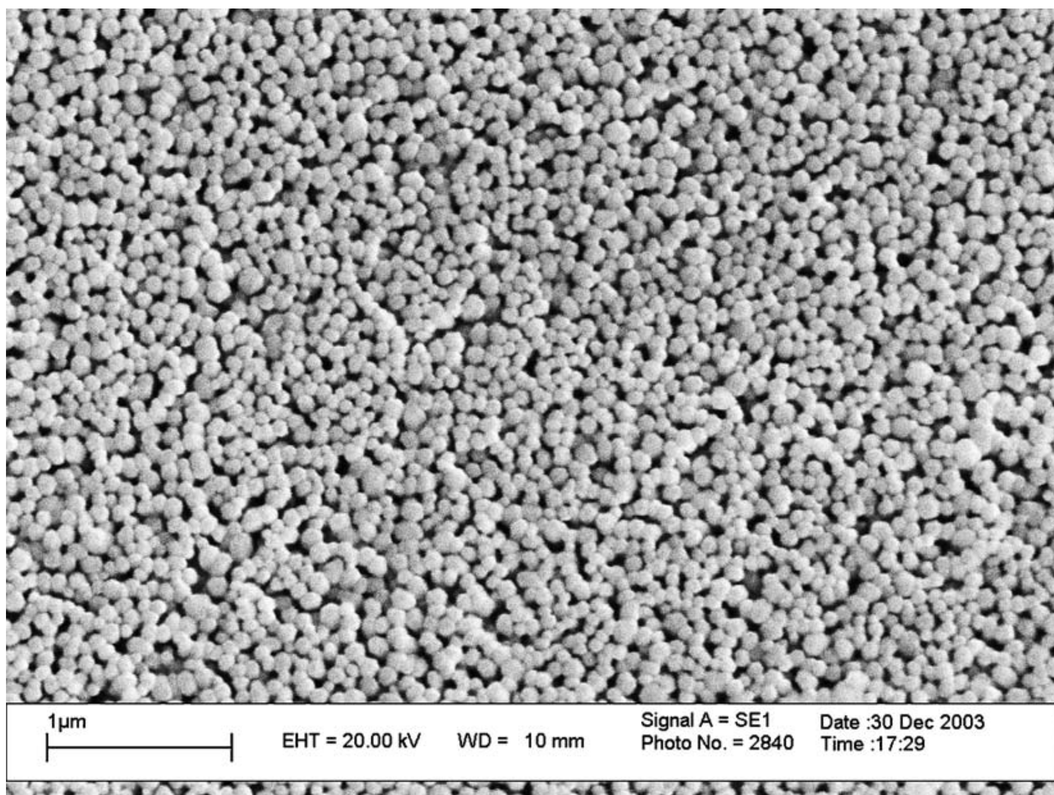

(f)

Figure 2 (*Continued*).

its motion on the surface, an adatom may meet others, with which they may react to form nuclei of critical size. Once stable nuclei are formed, they capture more adatoms, forming island. If the surface mobility is high, the islands merge while still very thin, forming a continuous film. At low sputtering power (Fig. 2a and b), adatoms with low kinetic energy result in negligible surface diffusion. The films hence appear non continuous with voided boundaries. At higher sputtering power (Fig. 2d–f), the Cu films appear to be continuous with no voided-boundaries. The fine round features observed in Fig. 2d–f are due to polycrystalline film structure. These small features were reported earlier [16] as grains after the comparison made between

the High Resolution SEM and TEM characterization result. The Cu film structure with fibrous grains appears at high sputtering power infers that the highly energized inert Ar ions provides translational kinetic energy to the adatoms. The surface diffusion of these adatoms was then enhanced with the momentum transfer to the growing surface. Where adatoms diffusion length becomes larger than distance between cluster sites, voided boundaries become filled by diffusing adatoms, and the film develops the characteristics void-free grain structure. Muller [19] in his modelling work done in 1988 has identified "higher impact mobility" and "forward sputtering" as two dominant mechanisms as the ways in which energy enhancement prevents or reduces the voided boundaries formation. "Higher impact mobility" was described by Muller as the phenomenon of higher adatom energy amounts to a high surface diffusion rate for few atomic distances on the film surface until the excess kinetic energy upon impact becomes dissipated into the bulk. Another mechanism, "forward sputtering" refers to momentum transfer from the approaching adatom (to the film surface) to the adatom already resides on the film surface causes the latter to be knocked loose and scattered forward. This in turn improves the surface diffusion and reduces the voided boundaries. We believe these two insight mechanisms of surface diffusion contribute to our Cu film void-free grain structure. The increase in the grain size as a result of bombardment to the growth surface by more energetic particles with increasing sputtering power has been reported by Song *et al*. [15b].

The effect of sputtering power on the electrical properties of Cu films grown at constant deposition pressure was shown in Fig. 1. The films resistivity observed in Fig. 1 decrease exponentially with the sputtering power. For films deposited at 75 W and higher, the film resistivity decreases gradually with the increase of the sputtering power with lowest resistivity of 3 μohm-cm occurring at highest sputtering power of 150 W. The gradual decrease in the resistivity for Cu film grown at 100 W and higher sputtering power is believed as the film resistivity approaching the constant resistivity at prescribed sputtering power. Below critical power 75 W, the film resistivity shows an increase to 34 μohm-cm at 50 W and increase rapidly to 84 μohm-cm at lowest sputtering power of 25 W. The possible factors contribute to the considerable increase of film resistivity at lower sputtering power (<75 W) are size effect owing to thinner film [20] grown at lower sputtering power, and reduced surface and bulk diffusion (surface mobility) due to the low adatom energy which results in low crystallinity [21]. These factors were similarly suggested by Cheng *et al*. [22a] as the reasons for the decrease in the film resistivity with the increase in sputtering power. In our case however, we rule out size effect as the size effect dependent film resistivity applies only to the film with thickness approaching mean free path of the current-carrying electron [23]. The increase in film resistivity at lower sputtering power in our experiment is attributed to voided boundaries film structure of low crystallinity owing to the low surface mobility, as manifested in our SEM micrographs (Fig. 2a and b). The better crystallinity achieved with higher sputtering power due to larger impact energy of the bombarding particles, which leads to better surface mobility has been reported by Hwang *et al*. [18b] and Cheng *et al*. [22b]. Also, Bellakhder et *al*. [24] reported the improve in crystallinity as the sputtering power increases. To demonstrate this, Fig. 3 shows the effect of voided boundaries on its electrical properties with the plots of Cu film thickness versus resistivity at (i) varied sputtering power (ranging from 25 to 150 W) and (ii) constant sputtering power (125 W). Comparison between these two curves shows that those Cu

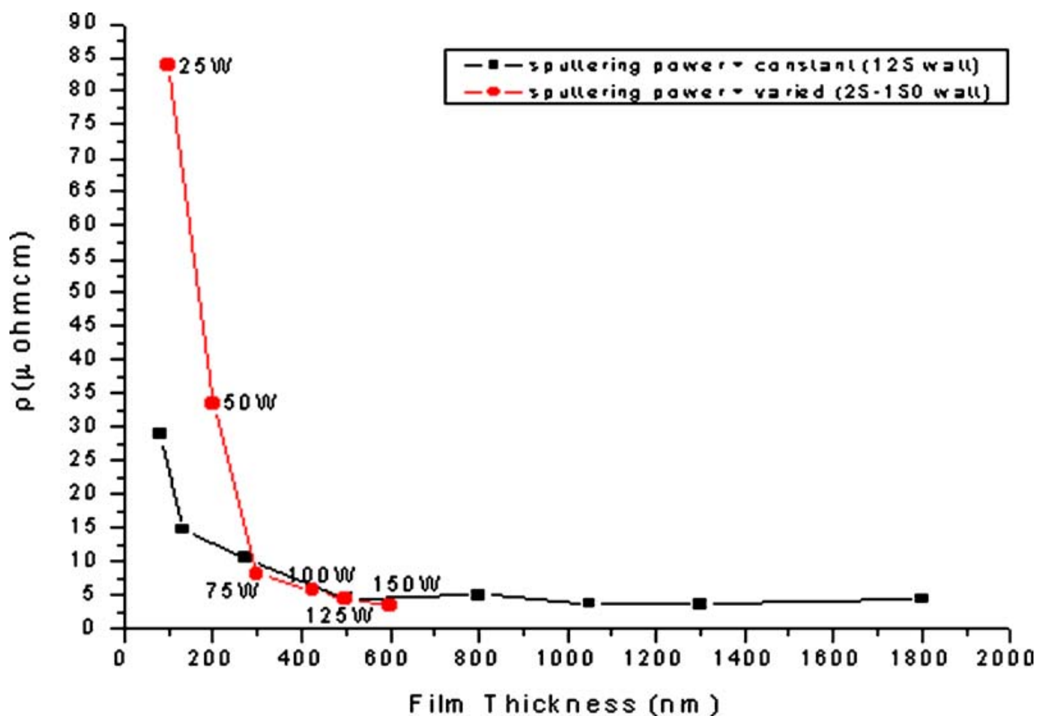

Figure 3 Film thickness versus resistivity at constant sputtering power and varied sputtering power.

films grown at lower sputtering power (<75 W) exhibit higher resistivity compared to film of similar thickness but grown at higher sputtering power (125 W). Conversely, the Cu films grown at higher sputtering power (150 W) exhibits lower resistivity compared to film grown at 125 W. The implication entailed from these is the lower constant resistivity can be achieved for lower thickness film at high sputtering power. Similar conclusion has been drawn by Shivaprasad *et al.* [21] for their work done on investigating the effect of deposition rate on the electrical resistivity of evaporated thin manganese films. They concluded from series of experiments involving manganese films of same thicknesses but grown at different deposition rate that the constant resistivity for manganese films obtained at lower thickness is attributed to higher deposition rates. According to Shivaprasad *et al.*, this high deposition rate gives rise to smaller islands with a higher rate of formation, which means a continuous film with less defect density is produced at lower thickness. The increase of film resistivity owing to the inter-granular void was recently reported by Arun *et al.* [25] for Sb_2Te_3 polycrystalline film. For higher sputtering power results in lower resistivity, it should be noted that there is a limit in the increase of sputtering power for the deposition rate and electrical properties optimization. This is because the deposition rate should not exceed a limit such that the overgrowing layer is deposited before atomic jump to an equilibrium position is possible, which will then result in non crystalline nuclei [26] formed on substrate surface, which exhibit high resistivity.

3.2. Deposition pressure effects on electrical & structural properties

Fig. 4 shows that the Cu film deposition rate decreases almost linearly with the deposition pressure ranging from 3.6 mTorr to 30 mTorr at constant dc sputtering power (100 W). At low deposition pressure of 1 mTorr, the Cu film deposition rate was observed to be lower than that of 3.6 mTorr. This phenomenon is due to inherent limitation with the deposition system employing non-high strength (HS) magnetron, which is unable to sustain the plasma at the prescribed low deposition pressure, resulting in lower deposition rate. The fact that the magnetron discharged at low Ar gas pressure in the range of $\sim\times 10^{-4}$ Torr requires modified magnetron to achieve high field strength has been reported earlier [27a, 28]. At deposition pressure of 3.6 to 10 mTorr, the deposition rates are about 40 nm/min. As the deposition pressure increases to 20 mTorr, the deposition rate decreases to 35 nm/min and at 30 mTorr, the deposition rate decreases to 30 nm/min. The decreasing deposition rate with the increase of deposition pressure as observed in our experiment is due to collision scattering events between the sputtered off Cu atoms and the Ar species in the deposition chamber. At 30 mTorr, the MFP (λ), defined as the mean distance that a particle travels in a gas before encountering a collision with a gas molecule in the sputtering chamber was about eightfold shorter than that of 3.6 mTorr. The chances of the sputtered-off Cu atoms collide with the excessive amounts of Ar species present under high deposition pressure is high, as with the relatively shorter MFP. Hence, some of the Cu atoms are scattered away from the substrate, resulting in lower deposition rate. The decrease of deposition rate with the higher deposition pressure due to the decrease in the MFP was also reported by Minami *et al.* [29], Subramanyam *et al.* [30a], Andujar *et al.* [17] and Assuncao *et al.* [31].

Fig. 5 shows the plane view of SEM micrographs of Cu layer grown at various deposition pressure, ranging from 1 to 30 mTorr at 100 W. The SEM mircrographs of Cu film grown at 1 mTorr (Fig. 5a) and 3.6 mTorr (Fig. 5b) show a uniform grains structure with bigger grains in the case of 1 mTorr. As the deposition pressure increases to 10 mTorr (Fig. 5c), the grains

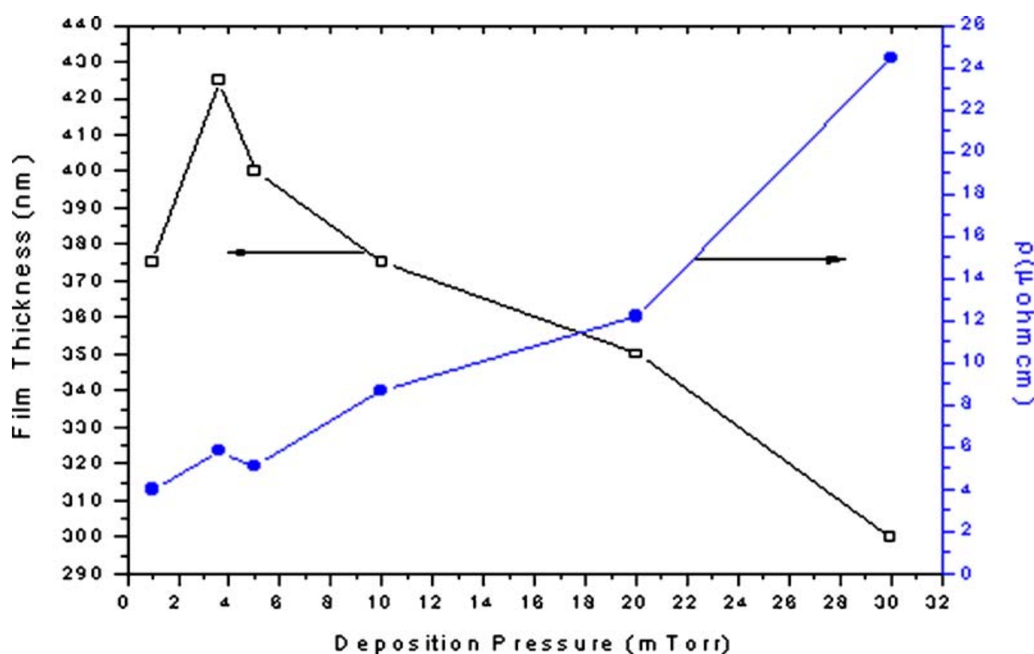

Figure 4 Deposition pressure effects on the film thickness and resistivity with deposition time 10 min. and sputtering power 100 W.

structure fades and the Cu film was observed to exhibit voided boundaries structure. As the pressure increases to 30 mTorr (Fig. 5d), there are more voided boundaries appear on the Cu films and these voided boundaries also appear to be wider. Similar observation on the voided boundaries structure of Cu film at high deposition pressure was reported by Joh *et al*. [16] for polyimide substrate. In the investigation, they reported that the voided boundaries appear to be more frequent as deposition pressure increases due to the shadowing effects. In our experiment, the transformation from the fine individually grains structure as observed in Fig. 5a

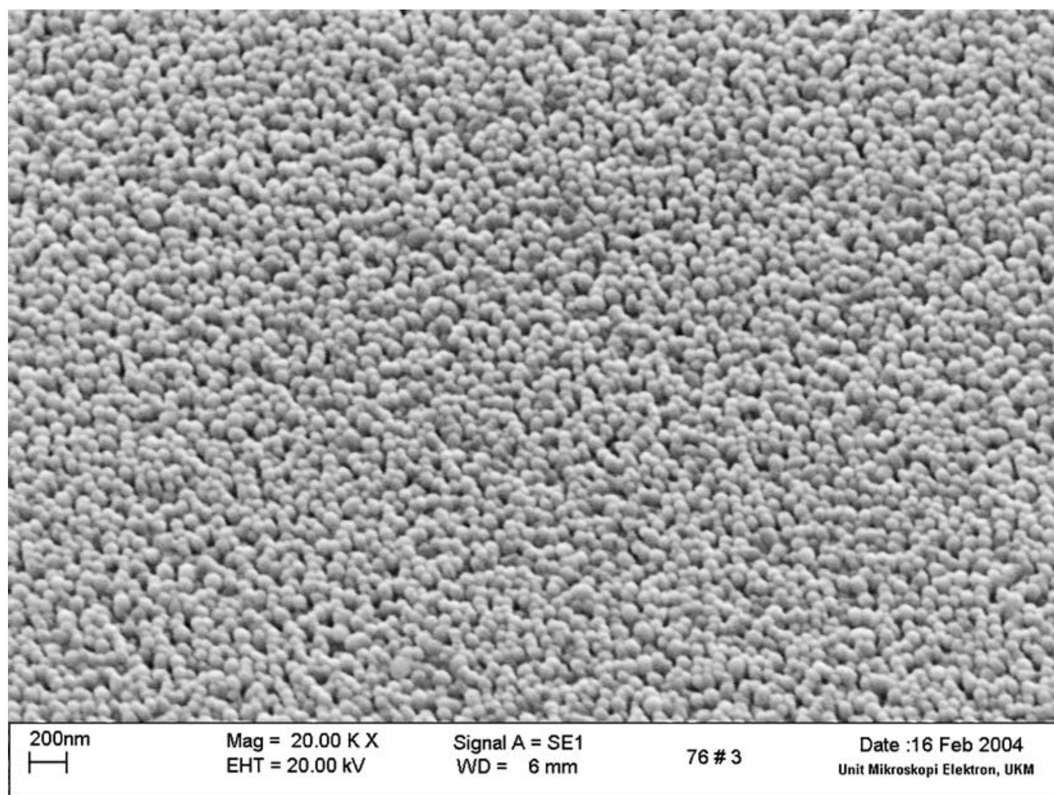

(a)

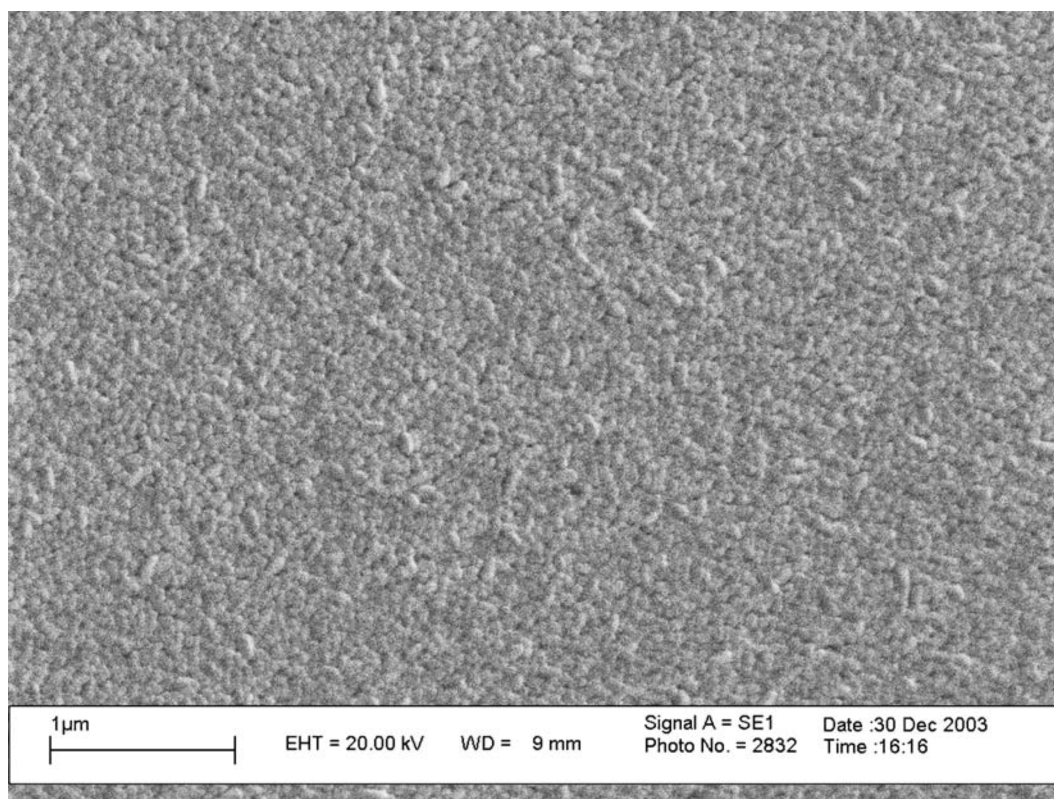

(b)

Figure 5 Plane view of SEM micrographs of Cu layer grown at: (a) 1 mTorr, (b) 3.6 mTorr, (c) 10 mTorr, (d) 30 mTorr on silicon substrate. (Magnification = 20.00 KX). (*Continued on next page*).

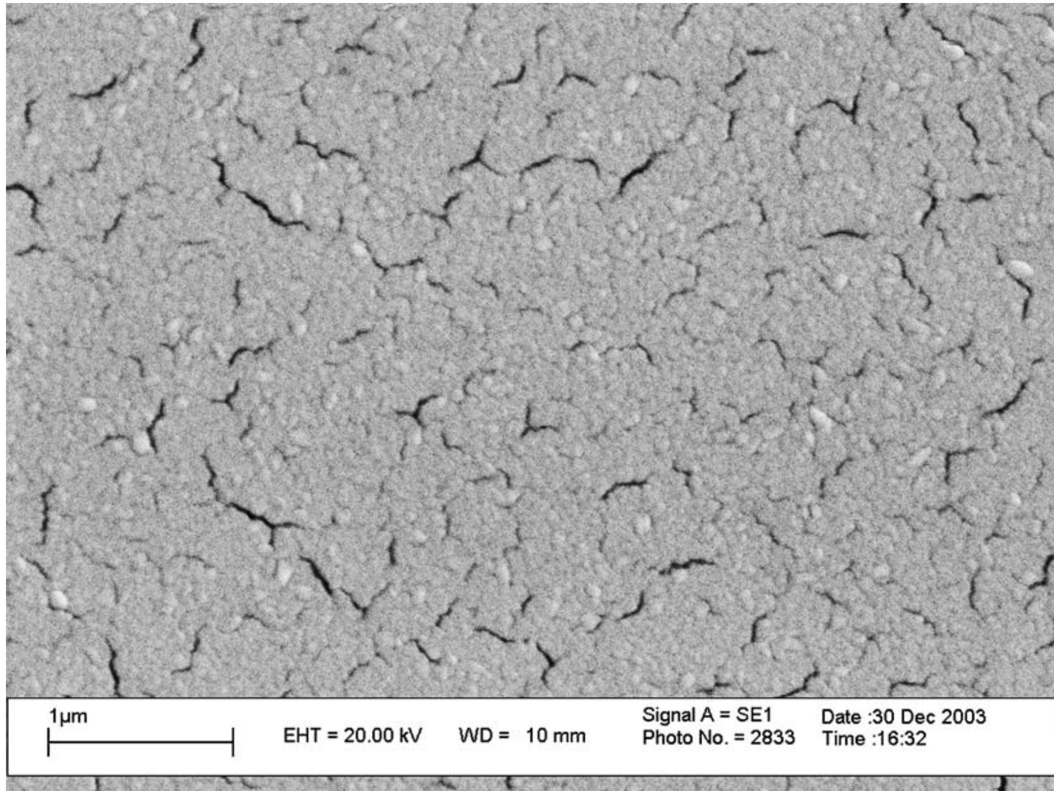

(c)

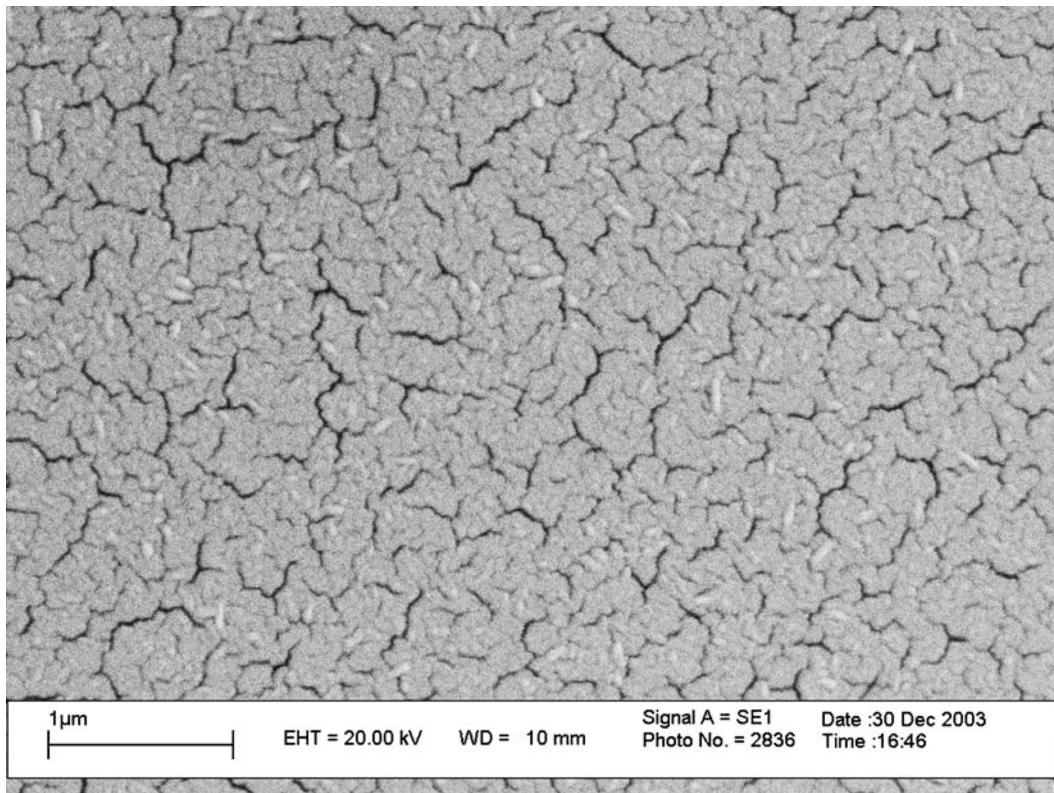

(d)

Figure 5 (*Continued*).

and b into voided boundaries structure in Fig. 5c and d is attributed to the decrease in the surface mobility of the adatoms after series of collisional events under high deposition pressure, as well as the similar shadowing effect, which is enhanced in the case of higher deposition pressure. The adatoms with higher energy under low deposition pressure are energetically favorable for the formation of fine individually grains. Assuncao *et al*. [31] has earlier reported the low surface mobility of the sputtered species after undergo collisions at high deposition pressure, which leads to tapered crystals separated by open, voided boundaries. Also, the decrease in the sputtering pressure results in the increase of the grain size due to increased kinetic energy

and surface mobility of the adatoms was reported by Cheng *et al.* [32]. Further to these, Igasaki *et al.* [33a] reported that increasing Ar gas pressure results in the decrease in grain size and increase in the grain boundary. The self-shadowing effect occurs during film deposition where the adatom cannot perch on top of each other, but rather settle sideways into the nearest "cradle" position, in which they establish relaxed bond lengths to their nearest neighbors. Because of the finite size of atoms, the "ballistic aggregation" can result in overhang structures, which shadow the low areas from deposition. Thereby, shadowing effect starts develop and even in perpendicular deposition, there develops shadowed voids between them. An increase in the inert gas pressure (deposition pressure) spread the range of incident angles and increased self-shadowing, resulting in wider and more frequent voided boundaries.

The plot of film resistivity versus deposition pressure for Cu film grown at 100 W was shown in Fig. 4. At 1 mTorr and 3.6 mTorr, the Cu film resistivity is about 4 μohm-cm and 6 μohm-cm respectively. At elevated deposition pressure of 10 mTorr, the resistivity increases to 9 μohm-cm and at highest deposition pressure employed in the experiment, the film exhibits 24 μohm-cm. Mikami *et al.* [27b], Song *et al.* [15b] and Igasaki *et al.* [33b] reported the similar dependence relationship between the film resistivity and deposition pressure. The generally increasing resistivity with the increase in deposition pressure ranging from 1 mTorr to 30 mTorr as shown in Fig. 4 is due to structural change of Cu morphology from grains structure at low deposition pressure to non continuous film with voided boundaries at high deposition pressure, which means degrade in the film crystallinity. The dependence relationship between the grain size and the crystallinity of the film has been reported by Subramanyam *et al.* [30b].

4. Conclusions

In this work, the effects of the dc sputtering power and deposition pressure on deposition rate, microstructure and electrical properties of DC magnetron sputter-deposited Cu on Si were demonstrated. The experiment results show that the sputtering power and deposition pressure play an important role in optimization of the DC magnetron sputter-deposited Cu films. The higher the sputtering power, the more likely the film formed is of continuous and with higher crystallinity due to sufficiently high adatom mobility which helps to improve the surface and bulk diffusion. The surface and bulk diffusion enable the adatom settles at equilibrium site and reduce the open boundaries. The significant implication drawn from this is the constant film resistivity could be achieved at lower film thickness if the high sputtering power is employed. On the other hand, the lower deposition pressure generally favors the film grown by reducing the voided boundaries as the impinging sputter-off Cu atoms are believed to be neither become scattered into more oblique incident angles which will result in voided columnar structure, nor dissipate their kinetic energy in gas collisions which will decrease the deposition rate and hence surface mobility. We conclude that by proper control of the sputtering power and deposition pressure, the growth of the sputter-deposited Cu films on Si could be optimized in terms of their deposition rate and also electrical properties through the improved structural properties.

Acknowledgements

This work was supported by Multimedia University's Internal R&D Research Funding Cycle 1/2004 under grant No. PR/2003/0255.

References

1. N. BENOUATTAS, A. MOSSER, D. RAISER, J. FAERBER and A. BOUABELLOU, *Appl. Sur. Sci.* **153** (2000) 79.
2. J. VANCEA, F. HOFMANN and H. HOFFMANN, *J. Phys. Condens. Matter* **1** (1989) 7419.
3. H. JIANG, T. J. KLEMMER and J. A. BARNARD, *J. Vac. Sci. Technol. A* **16** (6) (1998) 3376.
4. D. DEPLA, J. HAEMERS and R. D. GRYSE, *Plas. Sour. Sci. Technol.* **11** (2002) 91.
5. Z. A. ANSARI, K. P. HONG and C. M. LEE, *Mater. Sci. Engng. B* **90** (2002) 103.
6. C. S. RYU, K. W. KWON, A. L. S. LOKE, V. M. DUBIN, R. A. KAVARI, G. W. RAY and S. S. WONG, in "Symposium on VLSI Technology", Digest of Technical Papers (Honolulu, Hawaii, June 9–11, 1998).
7. Y. B. PARK and S. W. RHEE, *J. Vac. Sci. Technol. B* **15**(6) (1997) 1995.
8. W. H. TEH, L. T. KOH, S. M. CHEN, J. XIE, C. Y. LI and P. D. FOO, *Microelectr. J.* **32** (2001) 579.
9. P. BAI, G. R. YANG, L. YOU, T. M. LU and D. B. KNORR, *J. Mater. Res.* **5**(5) (1990) 989.
10. P. BAI, G. R. YANG and T. M. LU, *Appl. Physi. Lett.* **56**(2) (1990) 198.
11. P. BAI, G. R. YANG and T. M. LU, *J. Appl. Phys.* **68**(7) (1990) 3619.
12. (a) S. A. CAMPBELL, in "The Science and Engineering of Microelectronic Fabrication" 2 ed., (Oxford University Press, New York, 2001) p. 308; (b) *Idem.*, in "The Science and Engineering of Microelectronic Fabrication" 2 edn, (Oxford University Press, New York, 2001) p. 312.
13. J. E. MAHAN, in "Physical Vapor Deposition of Thin Films" (Wiley Interscience, New York, 2000) p. 178.
14. E. GAGAOUDAKIS, M. BENDER, E. DOULOUFAKIS, N. KATSARAKIS, E. NATSAKOU, V. CIMALLA and G. KIRIAKIDIS, *Sens. Actuat. B* **80** (2001) 157.
15. (a) Y. S. SONG, J. K. PARK, T. W. KIM and C. W. CHUNG, *Thin Solid Films* **467** (2004) 118; (b) *Idem.*, *ibid.* **467** (2004) 120.
16. C. H. JOH, J. G. JUNG and Y. H. KIM, *Korean J. Electr. Microsc.* **29**(3) (1999) 265.
17. J. L. ANDUJAR, F. J. PINO, M. C. POLO, A. PINYOL, C. CORBELLA and E. BERTRAN, *Diam. Related Mater.* **11** (2002) 1008.
18. (a) D. K. HWANG, K. H. BANG, M. C. JEONG and J. M. MYOUNG, *J. Crys. Gr.* **254** (2003) 451; (b) *Idem.*, *ibid.* **254** (2003) 452.
19. K-H. MULLER, *J. Vac. Sci. Technol. A* **6** (1988) 1690.
20. V. D. DAS and P. G. GANESAN, *Sol. State Comm.* **106**(5) (1998) 318.
21. S. M. SHIVAPRASAD and M. A. ANGADI, *J. Phys. D: Appl. Phys.* **13** (1980) L158.
22. (a) F. X. CHENG, C. H. JIANG and J. S. WU, *Materi. Des.* **26** (2005) 372; (b) *Idem.*, *ibid.* **26** (2005) 371.
23. J. W. LIM, K. MIMURA and M. ISSHIKI, *Appl. Surf. Sci.* **217** (2003) 96.
24. H. BELLAKHDER, A. OUTZOURHIT and E. L. AMEZIANE, *Thin Solid Films* **382** (2001) 31.

25. P. ARUN and A. G. VEDESHWAR, *Mater. Res. Bull.* **38** (2003) 1932.
26. A. WAGENDRISTEL and Y. WANG, in "An Introduction to Physics and Technology of Thin Films" (World Scientific, Singapore, 1994) p. 37.
27. (a) Y. MIKAMI, K. YAMADA, A. OHNARI, T. DEGAWA, T. MIGITA, T. TANAKA, K. KAWABATA and H. KAJIOKA, *Surf. Coat. Technol.* **133/134** (2000) 295; (b) *Idem.*, *ibid.* **133/134** (2000) 299.
28. J. H. BOO, M. J. JUNG, H. K. PARK, K. H. NAM and J. G. HAN, *Surf. Coat. Technol.* **188/189** (2004) 724.
29. T. MINAMI, S. IDA and T. MIYATA, *Thin Solid Films* **416** (2002) 93.
30. (a) T. K. SUBRAMANYAM, B. SRINIVASULU NAIDU and S. UTHANNA, *Cryst. Res. Technol.* **35** (2000) 10 1195; (b) *Idem.*, *ibid.* **35** (2000) 10 1196.
31. V. ASSUNCAO, E. FORTUNATO, A. MARQUES, H. AGUAS, I. FERREIRA, M. E. V. COSTA and R. MARTINS, *Thin Solid Films* **427** (2003) 402.
32. H. CHENG, Y. SUN and P. HING, *ibid.* **434** (2003) 115.
33. (a) Y. IGASAKI and H. KANMA, *Appl. Surf. Sci.* **169/170** (2001) 511; (b) *Idem.*, *ibid.* **169/170** (2001) 510.

Received 23 December 2004
and accepted 4 April 2005